# Analysis of flood warning and evacuation efficiency by comparing damage and life-loss estimates with real consequences related to the São Francisco tailings dam failure in Brazil

André Felipe Rocha Silva[1], Julian Cardoso Eleutério[1]

[1]Department of Hydraulic and Water Resources Engineering (EHR/SMARH), Federal University of Minas Gerais (UFMG), Belo Horizonte, 31270-901, Brazil

*Correspondence to*: Julian Cardoso Eleutério (julian.eleuterio@ehr.ufmg.br)

**Abstract.** Economic damage and life-loss estimates provide important insights for the elaboration of more robust alerts and effective emergency planning. On the one hand, accurate damage analysis support decision-making processes. On the other hand, the comparison of different flood alert scenarios through modelling technics is crucial for improving the efficiency of alert and evacuation systems design. This work evaluates the use of flood damage and life-loss models in floods caused by tailings dams through the application of these models in the real case of the São Francisco dam failure, which occurred in January 2007 in the city of Miraí, in Brazil. The model results showed great agreement with observed damage and loss of life. Furthermore, different simulations were done in order to measure the impact of increasing and decreasing alert system efficiency on life-loss reduction. The simulated scenarios exploring the inefficiency of flood alert and evacuation revealed that life-loss could have reached the maximum rate of 8.7 % of the directly exposed population when considering the more pessimistic and uncertain scenario instead of the null actual life-loss achieved. The results of this work indicate that the models were able to represent both, the observed accident and to represent different alert/evacuation efficiency impacts. It highlights the importance of developing and implementing robust alert and evacuation systems and regulations in order to reduce flood impacts.

## 1 Introduction

The benefits provided to society by the construction of dams of different types and purposes are undeniable. However, the failure of these structures may represent high damage potential to downstream valleys (Proske, 2018). From 1915 to 2022, a total of 257 tailings dams in the world suffered accidents accounting for 2,650 fatalities (Piciullo et al., 2022). The rate of tailings dam failures (1.2 %) is higher by two orders of magnitude than the value of 0.01 % reported for conventional dams (ICOLD, 2001; Azam and Li, 2010). In addition to the fact that tailings dams are historically more vulnerable than conventional dams (Rico et al., 2008a), these dams generally present a much more significant risk to the environment due to the physicochemical characteristics of materials that may be stored in their reservoirs (Kossoff et al., 2014; Fernandes et al., 2016; Rotta et al., 2020; Guimarães et al., 2022).

North America and Europe are the continents with higher records of accidents involving these structures (Rico et al., 2008b; Azam and Li, 2010). However, from 2000 to 2023, Brazil alone accounted for 11 tailings dam accidents, with consequences of different orders (economic, socioenvironmental, and cultural). Three of these accidents took place in 2019, including the Brumadinho dam failure, where 270 victims, including dead and missing persons, were reported (Project Chronology of Major Tailings Dam Failures, 2023).

Potential flood impact assessment is an extremely effective tool for supporting emergency planning and decision-making processes (Apel et al., 2004; Merz et al., 2010). Specifically in flood events, the main social relevant impacts are loss of life and/or economic damage, which are both objectively quantifiable and more relevant in the public perception of disasters (Jonkman et al., 2003). Several methods are available for evaluating loss of life and economic damage related to floods. Extended literature reviews were realized by Merz et al., (2010) for flood economic damage evaluation and by Jonkman et al., (2016) for flood loss of life evaluation. Since then, other relevant studies and models were achieved for economic damage (Gerl et al., 2016; Bombelli et al., 2021) and loss of life evaluations (Huang et al., 2017; Li et al., 2019; Mahmoud et al., 2020; Ge et al., 2021, 2022; Jiao et al., 2022; Alabbad et al., 2023). In addition, recent computational advances and software developments allow the performance of more robust impact simulations (e.g., LifeSim and Life Safety Model). However, international studies that focused on tailing dams impact assessments are rare. Lumbroso et al. (2021) performed life-loss simulations related to Brumadinho (Brazil) tailings dam failure. No studies focused, jointly, on both tailings dam failure economic and loss of life assessments were identified. This is one of the main topics explored in this paper.

We analyse the rupture of the São Francisco mining tailings dam, in Miraí city, Minas Gerais State (Brazil). This accident took place in 2007. It caused several damages in the downstream valley, including the flooding of around 300 to 500 dwellings, generating economic and environmental losses. Although a high risk was observed, the identification of the hazard and evacuation procedures adopted during the event led to the absence of fatalities. This accident represents an opportunity for research purposes once it presents a particular case of efficiency of evacuation and it was the object of some important data gathering in national studies (Pimenta de Ávila, 2007; Rocha, 2015; Veizaga et al., 2017) and media coverage, which provides relatively detailed data concerning the real flood extents and its consequences.

Even when considering natural floods, there are few studies comparing damage estimates with actual surveys (Molinari et al., 2019). The application of predictive models for estimating impacts under these conditions is of great scientific interest. It allows for validating the use of models against observed data and estimating potential impacts in more or less favorable conditions with the success of the observed evacuation, through the simulation of hypothetical scenarios.

In this context, this paper evaluates how accurate life-loss and damage models may be for estimating tailings dam failure floods impacts and alert and evacuation efficiency for loss of life alleviation. Furthermore, it performs the application of models to estimate economic damage and loss of life together. In addition to the objective of representing the real accident, we simulated different scenarios for warning and evacuation, validating and comparing the results with actual observed data, revealing the benefits of using models to guide flood warning and evacuation systems implementation.

## 2 Case study - The Miraí accident in 2007

The São Francisco dam was a structure for storing tailings from the effluent generated in the bauxite washing process of
65 *Mineração Rio Pomba Cataguases Ltda*. The dam was located eight kilometers from the urban center of Miraí, a city located
in the Zona da Mata of Minas Gerais State (Figure 1). This city was directly impacted by the breach wave. The São Francisco
tailings dam reservoir was 34 meters high, with a length of 90 meters, a width of 9 meters, and a capacity of approximately
3.8 million cubic meters.
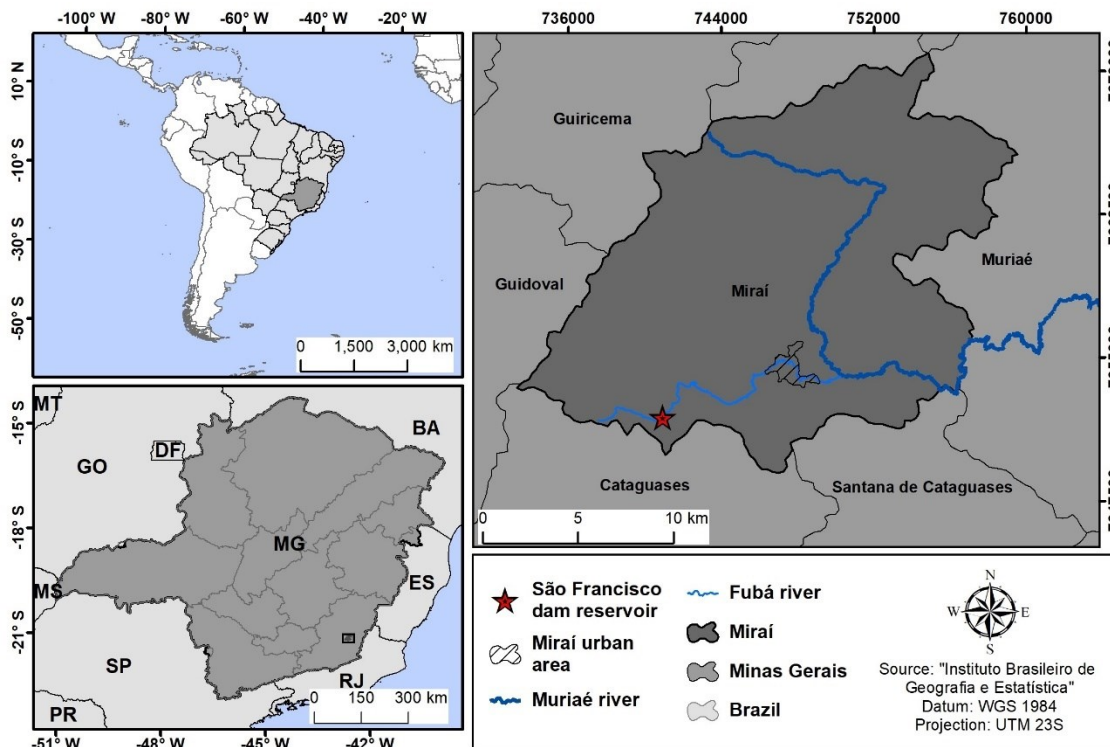
70
**Figure 1:** Location map of the São Francisco Dam in Miraí city (MG) – Brazil.

The Miraí accident occurred on January 10, 2007, and its description, with all available details concerning flood wave
propagation, reservoir characteristics and impacts, was obtained from Rocha (2015). At around 3:00 a.m., the water level in
75 the reservoir rose rapidly due to an intense rainfall of 121.3 mm, which lasted four hours. The water overtopped the crest of
the dam, starting to overflow through the surface spillway and through the contact of the massif with one of the dam abutments,
causing the dam to collapse due to the rapid erosion caused by the volume and speed of the water. According to local estimates,
the collapse began around 3:30 a.m., with a sharp increase in the breach until 5:30 a.m. that day. About 82 % of the volume of
mud stored in the reservoir spread through the Fubá River (which crosses the urban area of Miraí city) and continued beyond

80    the confluence with the Muriaé River. Figure 2 shows the Miraí accident and the extent of the observed inundation area, outlined using satellite images and aerial photographs.
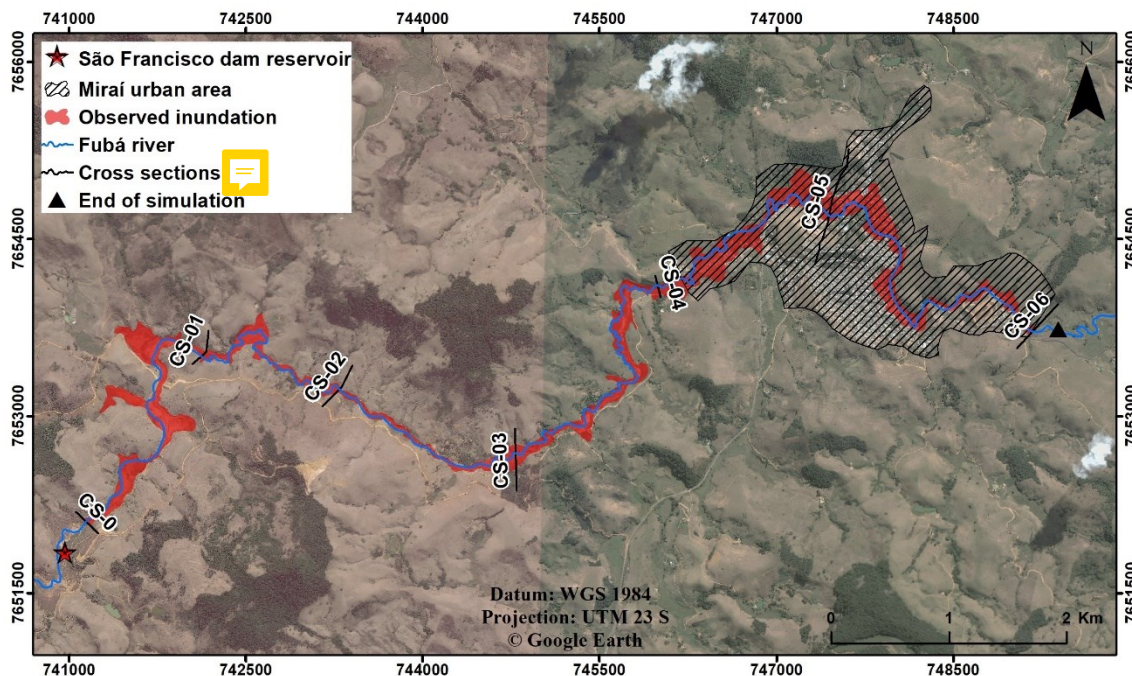
**Figure 2:** Observed inundation area after the São Francisco dam breach, Miraí – MG.

85

According to local studies, during the rainfall event period, the dam watchman noticed the rapid rise in the water level in the structure and notified the Military Police about the imminent danger of rupture when the water level of the reservoir was about 30 cm from the crest of the dam. After receiving the warning, approximately at the same time as the beginning of the dam collapse, the local Military Police went through the streets of Miraí city, helping on the successful evacuation of the whole

90    population during the night. Regarding the economic damage to the infrastructure of the city, the municipal government estimated a value of approximately 74 million reais (14.149 million dollars, using the average exchange rate for the first half of 2022 with a value of 5.23), which is around nine times the city's annual budget. This estimate did not include the damage to residents due to the loss of personal objects, furniture, and household structure. Other consequences of the event were the death of fish and the interruption of water supply in several cities downstream.

95    **3 Method for achieving the potential evaluation of flood impacts**

There are several methods for analyzing and quantifying economic damage (Merz et al., 2010). Nevertheless, due to the difficulty in specifying indirect and intangible damage, the methods usually focus on direct tangible damage. For estimating

this type of damage, Merz et al. (2010) consider the following aspects: characterization and classification of assets at risk; quantification of impacts on flood-exposed assets at risk; and association of the potential damage to assets through the use of damage models which relates assets typology and flood characteristics to damage economic potential.

The methods for assessing loss of life rely on behavioral assessment and macroeconomic indicators (Jongejan et al., 2005). However, the monetary specification of loss of life is complex due to the intangible characteristic of this type of damage. Risk assessments usually address fatalities directly and quantitatively, without monetary attribution (Jonkman et al., 2003). Potential quantification of direct loss of life comprises three main factors: first, the number of people potentially at risk; then, the effectiveness of evacuation and shelter strategies, thus determining the number of people who may be exposed to the event; and, finally, the fatality rate estimate, which is the ratio between the number of fatalities and the number of flood-exposed people (Jonkman et al., 2008). These main factors are represented by many other specific factors (e.g., flood and people characteristics and when the flood occurred) depending on the model.

There are several available life-loss models in the literature, as presented by Jonkman et al. (2016). Among these models, we highlight LifeSim (Aboelata and Bowles, 2005), which is an agent-based model, used in this research. LifeSim simulates the outcomes of event exposure, and its methodology links the loss of life to the evacuation of people or their success to find a safe shelter. Besides the model allows the estimation of economic damages. The full version of the model is integrated into HEC-LifeSim v.1.0.1 (USACE, 2018b). This version, which was developed by the U.S. Army Corps of Engineers (USACE), is the most used in North American consultancy and insurance companies (Needham et al., 2016), and it is being also widely used worldwide (Risher et al., 2017; Hill et al., 2018; Kalinina et al., 2018; Leong-Cuzack et al., 2019; Wang, 2019; Tomura et al., 2020; Bilali et al., 2021; Kalinina et al., 2021; Silva et al., 2021; Bilali et al., 2022). A more recent version, LifeSim v.2.0, has been implemented (USACE, 2021). However, some issues in this version, reported to the Risk Management Center (RMC) of the USACE prompted our decision to utilize the HEC-LifeSim v.1.0.1.

Based on these principles, the impact assessment methodology presented in this article consists of three parts: (1) using accident data to model the amplitude of the tailings flood wave, to map the flood extent, and to delimit the affected region; (2) estimating damage and loss of life based on the analysis of exposure and vulnerability of the urban area of Miraí city and the observed evacuation process; and (3) developing scenarios for warning and evacuation to estimate the efficiency of different measures that were or could be achieved during the flood event.

## 3.1 Dam breach modelling and flood wave mapping

In the HEC-RAS (Hydrologic Engineering Center - River Analysis System) model, the propagation of the flood wave is given by solving the Shallow Water equations (Brunner, 2021). In two-dimensional modelling using the HEC-RAS version 6.3, the channel and the floodplain were subdivided into nonoverlapping cells to form a grid for solving the equations. The digital elevation model (DEM) used to generate the numerical grid was obtained by the Shuttle Radar Topography Mission (SRTM), with one arc-second spatial resolution (30 meters). The Fubá river channel was inserted by using the AGREE method

130 (Hellweger and Maidment, 1997), with later correction of the river profile and insertion of topobathymetric points. This correction reduced the average error from 3.6 meters (DEM) to 1.2 meters (topobathymetric survey).

This grid can be structured by cells of any shape, with a maximum of eight faces. These cells can be orthogonal or not; however, if there is orthogonality in all or part of the grid, the solution of the applied numerical method has an advantage in computational speed. A hybrid discretization scheme that combines finite differences and finite volumes is used for solutions to Shallow

135 Water equations. Furthermore, the Shallow Water equations can be simplified, resulting in the diffusive wave model. However, simplification is not recommended for the present study since it addresses a dam failure, which denotes highly dynamic flood waves (Brunner, 2021). The variation in speed in these situations can be highly drastic in space and time, and diffusion wave simplification does not include the terms of local acceleration (change of speed over time) and convective acceleration (change of speed over space). The grid in this study was structured with 10-meter cells, being refined to five meters in the region of the

140 Fubá River channel (Figure 3). The Eulerian-Lagrangian Method was used to solve shallow water equations on flood propagation. The databases used for constructing the model and the maps were obtained by Rocha (2015) in a detailed local analysis of the accident.
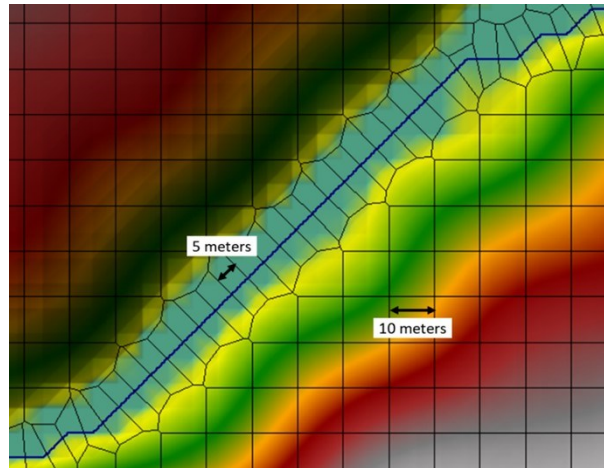
145 **Figure 3:** Structuring of the numerical grid used in HEC-RAS.

Through several experiments performed on mud flow samples, O'Brien and Julien (1985) defined classes of flow type by volumetric solid concentration. The authors noticed that the volumetric solid concentration in the waste stream is usually higher than 20 %. In these cases, there is a variation in fluid viscosity, the flow being considered non-Newtonian (Gildeh et

150 al., 2021). Some studies present techniques to model the flow resistance of non-Newtonian fluids (Jeyapalan et al., 1983; Jin and Fread, 1999; Rico et al., 2008a; Bernedo et al., 2011; Gildeh et al., 2021; Larrauri Concha and Lall, 2018; Piciullo et al., 2022). Studies on the applicability of some of these techniques (Travis et al., 2012; Melo, 2013; Martin et al., 2015; Rocha, 2015; Machado, 2017) demonstrate the capacity and limitations of tailings flood wave modelling adopting a Newtonian fluid.

For the case under study, analyses from a minor incident in 2006 during dam raising showed that the reservoir sludge had a volumetric solid concentration of 12 %, which consequently, allows the representation of the flow as aqueous according to the definition proposed by O'Brien and Julien (1985). Therefore, no technique was used to represent tailings flow resistance, without prejudice to the simulation.

As done for traditional flood modelling, different Manning coefficients were determined for each class of land-use and occupation determined by the Maximum Likelihood method, using Landsat 5 image (orbit 217 and point 75) of 10/15/2005, supplied by U.S. Geological Survey (USGS, 2005). The classes considered were (Figure 4): dense vegetation; sparse vegetation; exposed soil; urbanized area; and water body, with respective coefficients of 0.160; 0.035; 0.025; 0.100; and 0.040, as proposed by the Natural Resources Conservation Service (NRCS, 2016).
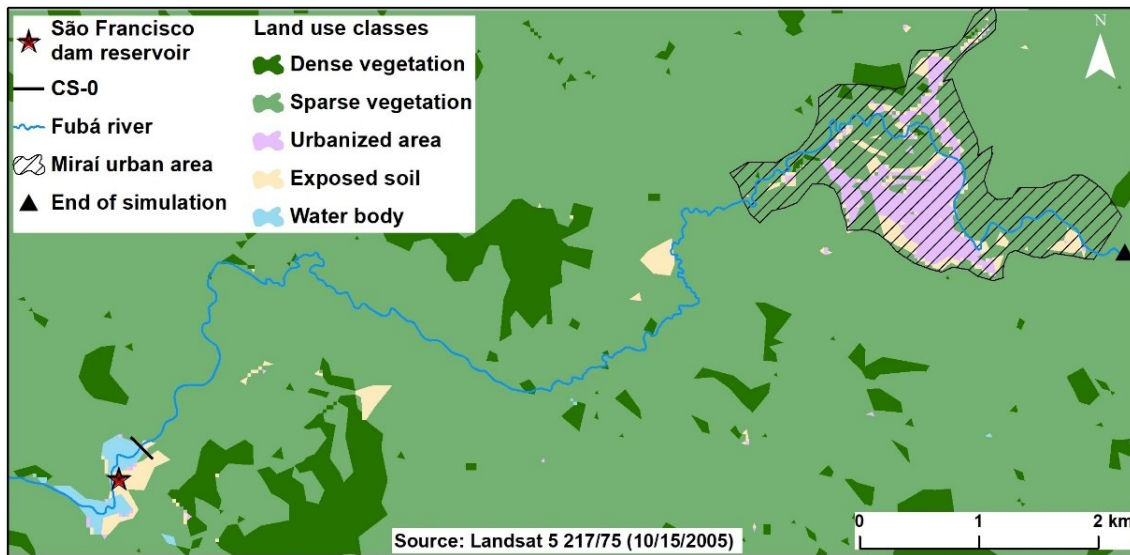
**Figure 4:** Map of land use and occupation - Manning coefficients.

The affluent hydrograph to the São Francisco dam reservoir was developed considering: the rainfall accumulation of 121.3 mm in four hours, the estimate of effective rainfall by the Curve Number (CN) method (NRCS, 1997), and the transformation of this effective rainfall into a runoff by the synthetic unit hydrograph method. The reconstruction of the accident (Rocha, 2015) led to the conclusion that the gap was 34 meters high, 70 meters wide at the top, and four meters wide at the bottom, and it developed in four and a half hours. Considering the affluent hydrograph calculated with a peak of 72 $m^3$ $s^{-1}$, the quota-volume curve, with 18 % of the material retained in the reservoir, and the quota-discharge curves of the spillway, the breach hydrograph was developed by the author starting at 03 h 30 min, with a peak flow of 422 $m^3$ $s^{-1}$, and peak and base time of 1 hour and 57 minutes and 3 hours and 54 minutes, respectively. This breach hydrograph was used as upstream boundary

175 condition of the model. As downstream boundary condition, normal depth was adopted in a section approximately 220 meters away from the urban area under analysis (the most fitted flow condition), not influencing the study area.

Regarding the spread of the tailings flood wave, the simulated inundation boundary comprised 1.171 km², equivalent to 89.4 % of the total observed (1.310 km²). Figure 5 shows the envelope of the simulated inundation area, highlighting the urban region of Miraí.

180
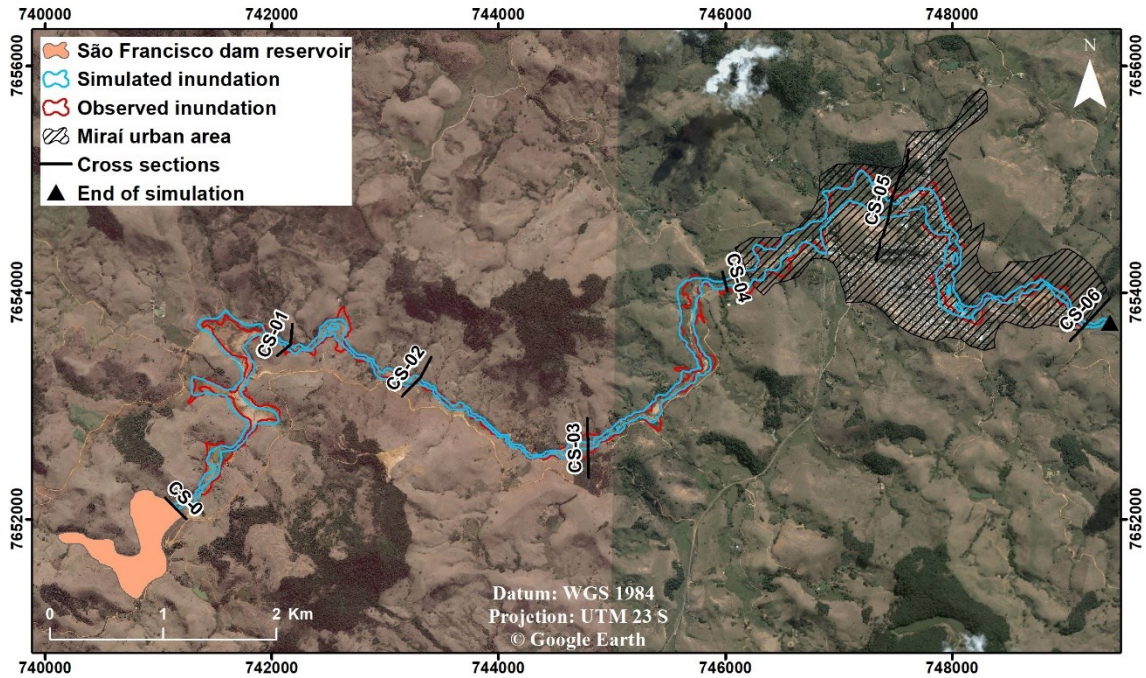
**Figure 5:** Inundation boundary simulated with HEC-RAS and observed from the São Francisco dam breach.

Despite having similar percentages, the inundation boundary shows noticeable differences. The simulation had area
185 overestimation and underestimation of 16.0 % and 26.3 %, respectively, when compared to the observed flood map. These discrepancies are a consequence of inaccuracies related to the DEM used, which tends to overestimate altimetry in areas with buildings and more robust vegetation, consequently reducing flood depths in these areas. Meanwhile, due to the low resolution of the model, the lack of details on altimetric obstacles that could obstruct wave propagation may lead to the overestimation of hydraulic parameters in flat areas (Paiva et al., 2011; Yamazaki et al., 2012; Saksena and Merwade, 2015; Jarihani et al.,
190 2015).

Analyzing the flood hydrograph propagation through the sections indicated in Figure 5, one can perceive greater damping of the peak flow in flatter regions. These regions provide an increase in flood wave spread in comparison to regions of high slopes with embedded valleys, which, in turn, provide higher propagation speeds (Figure 6). The reach between CS-0 and CS-01 comprises two large areas of flatland floodplain and an extensive floodplain. Such topographic characteristics are also observed

195     to a lesser extent in the stretch between CS-03 and CS-05. In turn, the reach between CS-01 and CS-03 comprises a high-slope region. In the urban region, between CS-05 and CS-06, there was no significant damping of the peak flow, only a delay in peak time. This is probably because the flood wave already reaches the urban area of Miraí city damped with low flow speeds. Table 1 presents the synthesis of the results for each cross-section analysed.
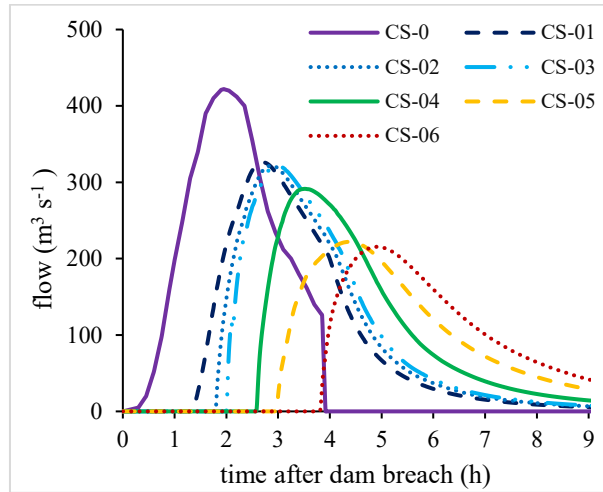
**Figure 6:** Breach hydrograph of the tailings wave propagation.

**Table 1:** Synthesis of the results of the tailings wave propagation.

| Cross section | Location downstream of the dam (m) | Peak flow (m³ s⁻¹) | Maximum depth (m) | Maximum speed (m s⁻¹) | Time of arrival (min) | Time to maximum depth (min) |
|---|---|---|---|---|---|---|
| CS-0 | 0 | 422 | 3.9 | 6.4 | 0 | 117 |
| CS-01 | 3,004 | 326 | 5.2 | 4.6 | 83 | 163 |
| CS-02 | 5,005 | 322 | 4.1 | 4.1 | 108 | 172 |
| CS-03 | 6,994 | 321 | 7.1 | 1.7 | 132 | 186 |
| CS-04 | 9,996 | 291 | 5.6 | 4.0 | 155 | 260 |
| CS-05 | 12,006 | 222 | 6.1 | 1.5 | 179 | 278 |
| CS-06 | 14,017 | 216 | 4.4 | 2.1 | 229 | 295 |

205     Even though some differences between simulation and observation were highlighted, the spread of the flood wave was consistent with the actual event that occurred in 2007. Witnesses reported that the evacuation in the first neighborhood of the

urban region took place at dawn. Table 1 shows that the time of arrival in the section closest to the start of the urban area (CS-04) occurs around 2.5 hours of the simulation, which is equivalent to 6:00 a.m. on the day of the event.

For the urban area of Miraí city, the object of the analysis of subsequent consequences, there were also discrepancies between the simulated and actual boundary (Figure 7). As for the entire study region, the simulated and the observed area differed noticeably, totaling 0.488 km$^2$ and 0.579 km$^2$, respectively. Area overestimation and underestimation in the simulation corresponded to 10.8 % and 26.5 %, respectively. Again, evidencing the consequences of inaccuracies related to the DEM used. Although there is a difference, it is important to note that the majority of the differences observed in terms of area are not highly relevant for the study's purposes. These differences are mainly observed in areas without buildings or population, with the exception of a central area where adaptations were made to improve the representation of the observed risk by addressing vulnerability and exposure.
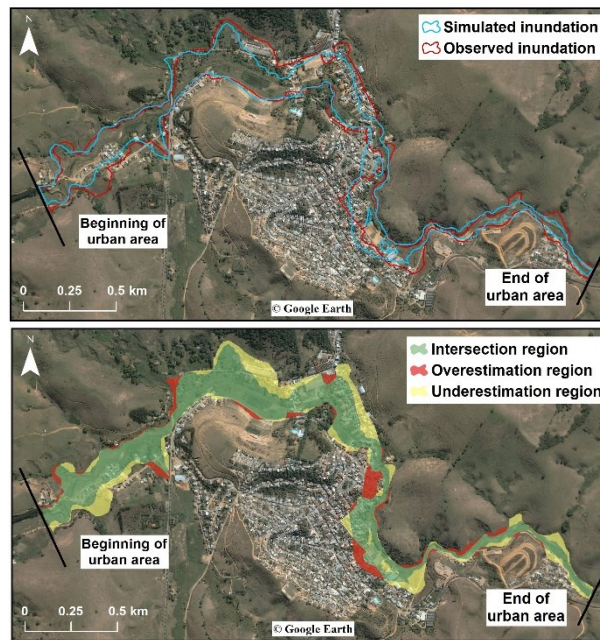
**Figure 7:** Cutout of the envelope of the inundation boundary simulated and observed from the São Francisco dam breach in Miraí city.

### 3.2 Potential damage and expected loss of life modelling

The agent-based life-loss estimation model used (HEC-LifeSim v.1.0.1) is structured using a modular modelling system (Zhuo and Han, 2020). In this system, each module exchanges information with other modules through a database that includes multiple layers and tables of the geographic information system (GIS). The model also presents the uncertainty module, which allows the insertion of uncertainty boundaries in several input parameters. Propagation of these uncertainties occurs with Monte Carlo simulations. The four modules present in the methodology are: "flood routine", which contains a set of networks

representing flood characteristics throughout the inundated area and period; "shelter loss", which simulates the exposure of
people and buildings during each event as a result of building submergence and potential structural damage; "warning and

230 evacuation", which simulates the distribution of the population at risk after the warning issuance; and "loss of life", which
estimates fatalities through probability distributions (USACE, 2018a). The inputs in the four modules are summarised in Table
2 and are further elaborated on below.

**Table 2:** Summary of HEC-LifeSim module inputs.

| Module | Input/Parameter | Data/Value |
|---|---|---|
| Flood routine | Hydraulic data | Dam failure flood modelling performed in HEC-RAS 2D |
| Loss of shelter | Structural inventory | Feature layer set by aerial images and characterized by the Brazilian demographic census |
| | Damage model | USACE (1985) for building stability criteria and Nascimento et al. (2007) for monetary damage estimation |
| Warning and evacuation | Hazard communication delay | Uniform distribution [-30, 0] minutes from dam failure starting |
| | Warning issuance delay | Triangular distribution (0, 15, 30) minutes |
| | Warning dissemination time and mobilization time | Figure 11 based on Sorensen and Mileti (2015b, 2015e) recommendations given the characteristics of the event |
| | Road networks | OpenStreetMap |
| | Destinations | Set in high places outside the extent of the floodplain and close to roads |
| | Pedestrian speed | 1.79 m s$^{-1}$ |
| | Vehicle speed | Maximum speed defined by the class of the road determined by the Census Bureau's Census Feature Class Codes and the speed on traffic conditions simulated by the modified transport model of Greenshields et al. (1935) |
| | Fraction of the people in vehicles | 0.5 |
| Loss of life | Fatality rates | Fatality distribution curves for chance, compromised and safe zones, obtained by McClelland and Bowles (2002) and updated by USACE (2018a) |

235

Exposure and vulnerability analyses were carried out to prepare an inventory of buildings presenting and characterizing the
structures and populations at risk in the flood-affected region. The following information was consolidated for buildings and

population in the shelter loss module: dwellings location, occupation type, construction material, number of floors, and population under and over 65 years of age (mobility criterion).

240   The affected population and number of households were determined by a set of regular statistical grids integrating data from different sources and aggregated in incompatible geographic units (IBGE, 2016). For each grid in the flood-affected region (Figure 8), households were geographically allocated with the aid of satellite images, and the population per household was considered homogeneously across the entire grid. Once the impacted area is majorly occupied by residential buildings and because the breach occurred during the night, outside business hours, other types of construction were not considered in the

245   study.
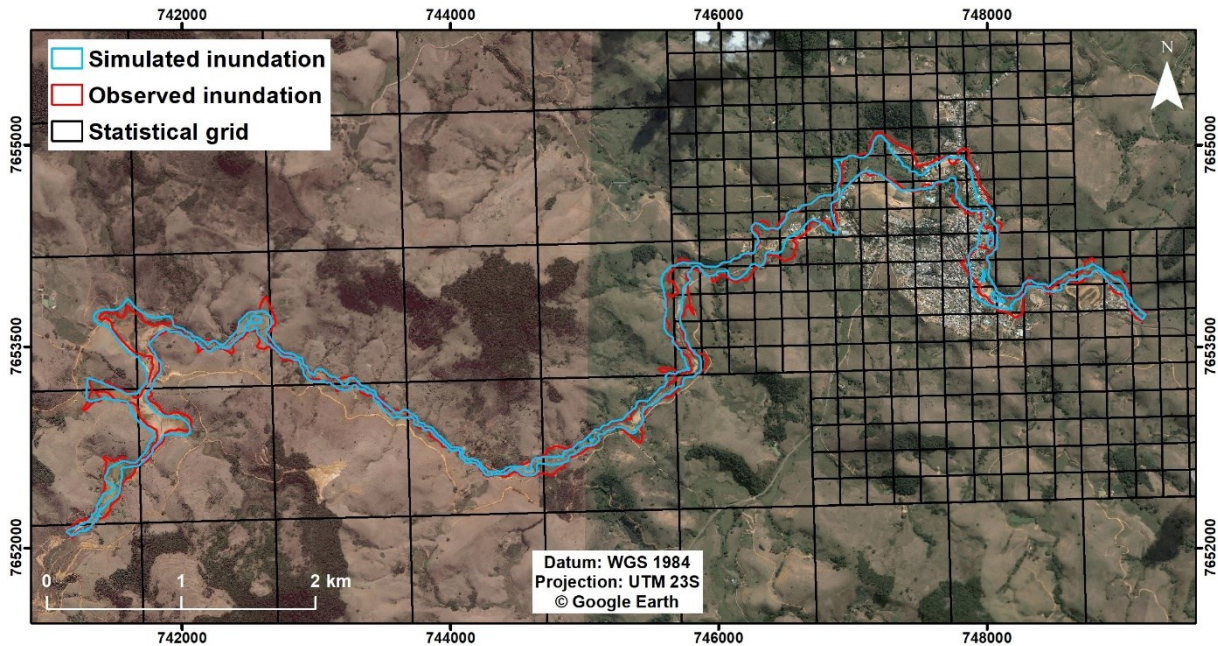
**Figure 8:** Statistical grid in the flood-affected region.

250   The exact number of buildings directly impacted by the flood wave in 2007 was not recorded. In local studies, it is possible to estimate that the number of buildings directly affected is between 300 and 500. The observed estimated flood boundary indicates that 358 households may have been directly affected (354 in the urban area and 4 in the rural area). The simulated flood boundary indicates 311 buildings (308 in the urban area and 3 in the rural area) (Figure 9).
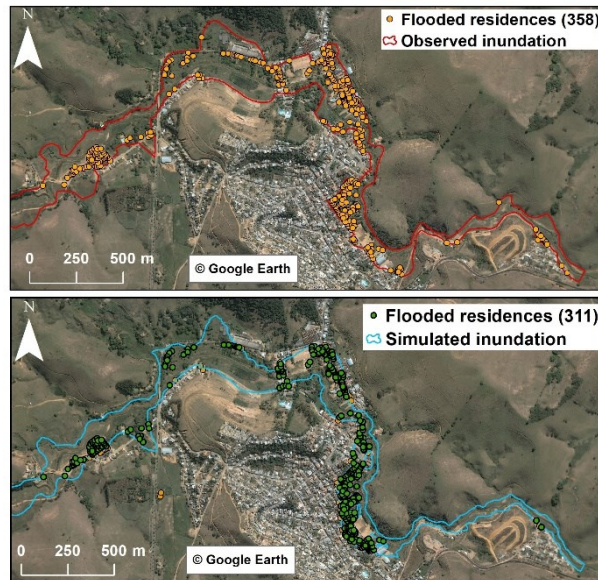
**Figure 9:** Zoom in the urban area of Miraí city indicates the households potentially affected by the observed and simulated inundation boundary.

To characterize households and the population obtained by the statistical grid, samples of households and people existing in the 2010 Brazilian Demographic Census microdata were used, which is the main reference for characterizing the population in Brazilian urban areas. For the confidentiality of research informants, the smallest geographic unit for identifying microdata is the weighting area, which is formed by grouping census sectors (IBGE, 2011). Therefore, the results obtained considering the weighting areas of interest were arranged proportionally and distributed evenly in the affected region. Each element of the sample was multiplied by its sample weight to represent the population.

The sample of households also enabled the determination of construction material, occupation type, and social class, which is essential for damage evaluation purposes. The construction materials considered were masonry and wood. Occupation types were adopted considering the building codes presented by Gutenson et al. (2018): single-family home (RES1); temporary accommodation (RES 4); institutional dormitory (RES 5); and asylum or orphanage (RES 6). The social class was defined using the average monthly family income defined for each class as proposed in the Brazil Economic Classification Criterion 2010 from the Brazilian Association of Research Companies (ABEP, 2012). The sample of people enabled the determination of the population under and over 65 years of age that were present at home at night, using the variable "return home".

Statistical grids showed that 1,537 households were affected by the flood, corresponding to a population of 4,675 people. The Microdata analysis considered the only weighting area existing for Miraí city. A total of 4,209 households were obtained in the considered weighting area, in which there is a predominance of single-family residential typology, masonry construction material, and social classes C and D (Table 3). The total population in the weighting area was 13,808, with 94.6 % being present at home at night (Table 4).

**Table 3:** Data obtained from the 2010 Brazilian Demographic Census microdata on households in the affected region of Miraí city.

| Type of data | Occupation type* | | | | Construction material | | Class** | | | |
|---|---|---|---|---|---|---|---|---|---|---|
| | RES1 | RES4 | RES5 | RES6 | Wood | Masonry | A | B | C | D |
| Microdata | 4,132 | 0 | 22 | 55 | 0 | 4,209 | 141 | 478 | 1553 | 2037 |
| % | 98.2 | 0.0 | 0.5 | 1.3 | 0.0 | 100.0 | 3.4 | 11.4 | 36.9 | 48.4 |
| Region of interest | 1,509 | 0 | 8 | 20 | 0 | 1,537 | 51 | 175 | 567 | 744 |

\* (RES1) single-family home; (RES 4) temporary accommodation; (RES 5) institutional dormitory; and (RES 6) asylum or orphanage, defined according to Gutenson et al. (2018).
\*\* Socioeconomic classes A, B, C, and D, with A being the highest and D the lowest, according to criteria established by ABEP (2012).

**Table 4:** Data obtained from the 2010 Brazilian Demographic Census microdata on the population in the affected region of Miraí city.

| Type of data | Population at home at night | | |
|---|---|---|---|
| | Total | < 65 years | > 65 years |
| Microdata | 13,062 | 11,724 | 1,338 |
| % | 94.6 | 84.9 | 9.7 |
| Region of interest | 4,422 | 3,969 | 453 |

By the analysis performed, the population at night directly affected was 1,033 and 868, for the extent of observed and simulated flooding, respectively. To minimize the possible effects of overestimating and underestimating the extent of the flood on the number of buildings and people directly affected, we constructed an alternative scenario of exposure and vulnerability analysis. In this scenario, the number of people allocated to the residences within the simulated inundation boundary was increased to equal the number of people affected according to what was found in the observed area. This excess number of 165 people was randomly allocated to the affected households according to the extent of the simulated flood, keeping the percentages in Table 4.

For building submergence in HEC-LifeSim, it is proposed three flood head limits physically defined by the interaction between existing shelter and depths thresholds: "chance zone", "compromised zone", and "safe zone". Chance zone refers to a condition where flood victims are typically swept downstream or trapped underwater, and survival depends largely on chance. Compromised zone refers to a condition where the shelter has been severely damaged, increasing the exposure of flood victims to violent floodwaters. On the other hand, the safe zone is typically dry, and the life-loss probability is virtually zero. For structural damage in buildings, stability is defined by speed and depth criteria, also considering occupation type, construction material, and the number of floors. HEC-LifeSim allows the use of several stability criteria, among these the criteria of USACE (1985) and RESCDAM, 2000).

The warning and evacuation module represents the distribution and behavior of the population during the flood event, including each emergency planning zone (EPZ) in the affected area. This process has several milestones that are separated by time lag intervals as shown in the timeline in Figure 10.

300
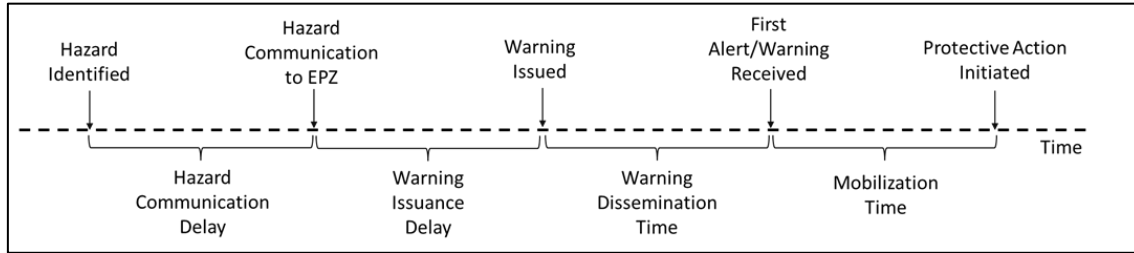
Figure 10: Warning and evacuation timeline.

**Source:** USACE (2018a)

305 The timeline starts from the identification of the imminent threat and presents the first delay in communicating the threat to managers. In both situations, there are no studies that assist in determining these values; therefore, the user must determine the time considering the characteristics of the case under study. In contrast, the choice of time in the other three subsequent delays is supported by the studies and equations of Sorensen and Mileti (2015a, 2015b, 2015c, 2015d, 2015e). These authors analysed many disaster cases with data available for evacuation, not only about floods but mainly about chemical and fire accidents,

310 adjusting models through the historical cases and defining coefficients to represent a certain type of existing warning system and population characteristics. Besides, in the identification of the threat and all delays, it is possible to insert uncertainty in the input data.

For the dynamics of evacuation, the modified transport model of Greenshields et al. (1935) is used to represent the effects of traffic density and road capacity on vehicle speed, and the short path algorithm of Dijkstra (1959) is used to determine the path

315 with the shortest travel time to the destination. The road network can be inserted by the user or imported directly by OpenStreetMap. If the vehicle or people are reached by the flood during the evacuation, the stability criteria defined by Aboelata and Bowles (2005) are used. If these criteria are exceeded, the affected population is allocated to the chance zone; if not exceeded, the population is allocated to the safe zone. Other evacuation parameters, such as the fraction of population in vehicles vs. on foot, are presented in Table 2.

320 For the representation of the warning and evacuation timeline, the delays for each step in Figure 10 were determined. Based on the information regarding the watchman's perception of the imminent danger before the breach, the period between the hazard identification time and the communication to the emergency planning zone was determined as a uniform distribution from 0 to 30 minutes before the dam breach. This interval corresponds to the period between the perception of the watchman and the start of the collapse of the dam. For warning issuance delay, a triangular probability distribution was adopted with the

325 minimum, most likely, and maximum values of 0, 15, and 30 minutes, respectively. The other two stages, with their respective

uncertainties, were defined through the relationship between the characteristics of the warning that occurred at the event and the recommendations of Sorensen and Mileti (2015b, 2015e). Figure 11 shows the 90 % confidence interval for the percentage of the population mobilized after the alert was issued (which is the sum of these last two delays). By the median, the entire population starts evacuating 150 minutes after the alert is issued.

330
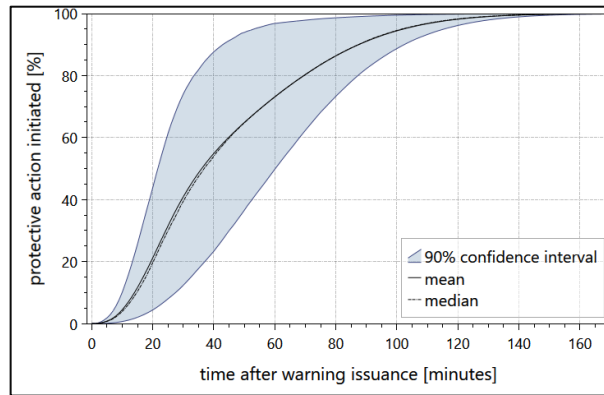
**Figure 11:** Combined dissemination and mobilization time for the evacuation scenario in the Miraí accident.

The fatality distribution curves, obtained by McClelland and Bowles (2002) and updated by USACE (2018a) through the
335 analysis of historical cases of mainly dam breach floods, were applied in the loss of life module. To determine the economic damage, the empiric national equations of Nascimento et al. (2007) were inserted in HEC-LifeSim for each social class affected by the flood. The curves relate the depth (h) in meters to the damage in R$ m$^{-2}$ (Reals per built projected area square meter) to the structure of the property and its contents. The built area of the affected households was estimated in the function of national social classes, as defined by Nascimento et al. (2006). Table 5 presents the equations and ranges of built area for each social
340 class. These equations were proposed in 2007 and for their use, it is need correction of the values by some inflation index.

**Table 5:** Model for economic damage and the most frequent range of built area as obtained by Nascimento et al. (2007) for each social class.

| Class | Damage (R$ m$^{-2}$) | Built area (m$^2$) |
|---|---|---|
| A | $90,832 + 39,334.\ln(h)$ | 200 – 250 |
| B | $103,938 + 43,844.\ln(h)$ | 100 – 150 |
| C | $74,685 + 27,388.\ln(h)$ | 50 – 100 |
| D | $18,049 + 33,364.\sqrt{h}$ | 25 – 75 |

345 After 1,000 interactions (value used in studies applying HEC-LifeSim), the economic damage was estimated at R$ 1.01 million to R$ 1.95 million for the 311 households affected directly by the simulated flood. Corrected by a factor of 169.12 % (based

on the Broad National Consumer Price Index – IPCA in June 2022), this value corresponds from R$ 2.72 million to R$ 5.23 million in 2022 (US$ 521 thousand to US$ 1.00 million).

According to the public registry, five hundred lawsuits related to property material damage were filed by residents against the mining company following the accident. Several of these lawsuits, judged between 2012 and 2013, resulted in indemnities ranging between 956 and 1,530 US dollars (STJ, 2014). Assuming that this indemnity range was allocated to each household and applying it to all 311 affected households, a range between R$ 1.56 million and R$ 2.49 million is obtained in 2012. By using the IPCA-based correction factor of 89,67 %, this value corresponds from R$ 2.95 million to R$ 4.72 million in 2022 (US$ 564 thousand to US$ 902 thousand). Thus, on average, this range of indemnity values was close to the simulated economic damages for households (between 4.64 and 8.92 thousand reais per household impacted according to the corrected value for the year 2012) (US$ 888 to US$ 1.71 thousand). Table 6 summarizes the results of flood economic damage estimation.

**Table 6:** Summary of economic damage, using the Broad National Consumer Price Index – IPCA to update the value to 2022.

| Value | Simulated damage in 2007 (million dollars) | Simulated damage in 2022 (million dollars) | Indemnities 2012 (million dollars) | Indemnities 2022 (million dollars) |
|---|---|---|---|---|
| Minumum | 1.01 | 2.72 | 1.56 | 2.95 |
| Maximum | 1.95 | 5.23 | 2.49 | 4.72 |

Regarding the estimated loss of life, the values obtained following the actual event, with a median of zero fatality. On average, 99.97 % of the population escaped the flood. Fatalities were estimated in only 67 of the 1,000 interactions, whose frequency of occurrence was: 1 fatality in 65 interactions; 2 fatalities in 1 interaction; and 3 fatalities in 1 interaction.

The successful evacuation of the population, with an average of 99.97 % of the population escaping the flood, is explained by the relationship between the flood timeline and the warning and evacuation. As demonstrated in the analysis of the spread of the tailings flood wave, the flood water reaches the beginning (CS-04) and end (CS-06) of the urban area in approximately 2.5 hours and 4 hours, respectively. Such periods were sufficient for mobilization to occur. Considering the most extreme negative combination of the times defined for the warning and evacuation process, the population is fully mobilized in approximately three hours.

For the alternative scenario of exposure and vulnerability, in 65 interactions fatalities were estimated, whose frequency of occurrence was: 1 fatality in 6 iterations; 2 fatalities in 58 iterations; and 3 fatalities in 1 iteration. This result indicates that the model fitted the real event and the difference in the population directly affected by the extent of observed and simulated flooding did not influence the estimated loss of life.

375 Furthermore, in all 66 iterations in the base scenario that resulted in one or two fatalities the loss of life concerned the population over 65 years of age, who was not mobilized for evacuation and, therefore, was allocated to some of the flood risk areas. The same result was noticed in 62 of 64 iterations in the alternative scenario. This behavior indicates the impact on the divergent submergence thresholds defined by Aboelata and Bowles (2005) to represent the mobility criterion. For the chance zone, the threshold is 4.58 m and 1.82 m for people under and over 65 years of age, respectively. As expected, the simulated

380 flood extent small uncertainty highlighted before showed to have no influence on the life-loss estimates.

### 3.3 Analysis of warning and evacuation efficiency

An effective warning system is dependent on several factors and is essential for selecting appropriate emergency management (Rogers and Sorensen, 1989; Lumbroso and Davison, 2018; Tonn and Guikema, 2018; Kolen et al., 2020). To assess the success of the warning and evacuation with a view to a good representation of the simulations in comparison with the observed

385 data, we developed, beyond the actual "optimistic" scenario that occurred, three more scenarios: "pessimistic", "moderate", and "unknown" (Table 7). The simulations were executed for both base and alternative scenarios of exposure and vulnerability. The period between the time of identification of the hazard and the communication to the emergency planning zone was considered null, and the three remaining steps, warning issuance delay, warning dissemination, and mobilization time (Figure 10), were defined through the recommendations of Sorensen and Mileti (2015a, 2015b, 2015e) for issuance and dissemination

390 of the warning and mobilization of the population.

**Table 7:** Description of each modelled scenario of warning and evacuation efficiency.

| Scenario | Description |
|---|---|
| Optimistic (actual) | It represents the real scenario that occurred in the event on January 10, 2007, and it is characterized by reports that detailed the accident, as described in section 3.2. In this scenario, the evacuation was successful, with the entire population mobilizing, on average, 150 minutes after the alert was issued. |
| Pessimistic | It represents the worst possible scenario, using limited alerting technologies. Therefore, any emergency response necessarily involves improvisation. Affected communities are unlikely to believe that they have a serious threat or that they may face events that require a rapid response. |
| Moderate | It represents an intermediate scenario, using only a combination of traditional technologies. About population, it indicates the situation that most represent a community given a mix of existing factors. However, it considers that this community does not have effective emergency planning. |
| Unknown | It represents a scenario in which the existing alert system in the affected region is unknown. Therefore, the range of uncertainty inserted in the stages of the alert and evacuation process is greater, resulting in expected high variability in the estimate of the loss of life. |

When simulating these three additional alert and evacuation scenarios, differences were found between the two exposure and
vulnerability scenarios (Figure 12). In all simulations the median of the alternative scenario was higher by 2 fatalities compared
to the base scenario: respectively for the base and alternative scenarios, it was computed 21 and 23 losses for the pessimist
alert/evacuation scenario, 13 and 15 losses for the moderate, and 15 and 17 losses for the unknown. In addition to verifying
the high impact of the level of efficiency of the alert and evacuation system, the observed and adopted optimistic scenario in
the evacuation process was confirmed in the real representation of the event that occurred in 2007. In all the standard curves
of Sorensen and Mileti (2015a, 2015b, 2015e) use to represent the delay in the issuance of the alert, the dissemination of the
alert, and the mobilization, the estimates of the loss of life were higher than those obtained throughout these scenarios.
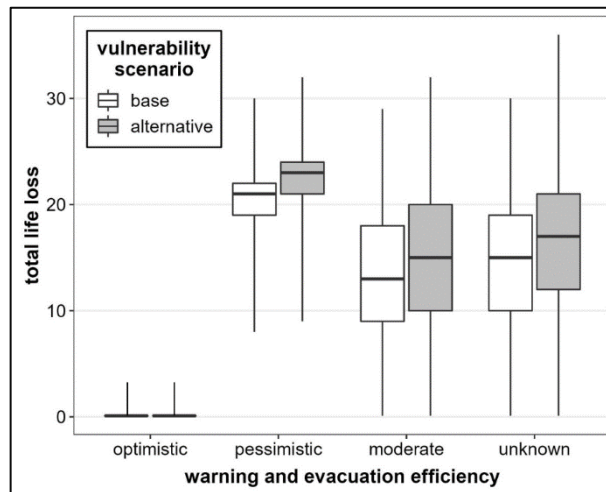
**Figure 12:** Life-loss estimation for different scenarios of warning and evacuation efficiency.

## 4 Conclusions

Risk assessment is an effective tool to assist in the emergency planning requested for tailings storage structures under Brazilian
law through. This work aimed to verify the application of consequence models by comparing their real and estimated outcomes
using the dam failure event that occurred in São Francisco Dam, in Mirai/Brazil, in 2007. It was possible to collect the real
event data mainly based on local technical reports and information collected from local authorities and post-event local studies.
The breach characteristics, arrival time at the city and the extension of the flood are examples of this data.
The hydrodynamic modelling showed satisfactory results mainly due to the similarity in the time the flood wave arrives, which
is one of the main parameters in loss of life modelling since it correlates with the time available for evacuation of the population
at risk. The modelling of the economic damage was similar to the indemnity values per household. The model was also capable
to represent the loss of life estimates and the success of evacuation in the event that occurred. However, in this specific case,
the low concentration of solids in the flow may have been one of the factors that contributed to the success of the results

obtained. We emphasize the need to carry out studies of this type for other real accidents with greater solid loads so as to expand the possibilities raised in this study.

For a priori analyses of dam failure consequences, the consideration of several uncertainties in flood modelling is ideal to better represent the event in flood risk assessment. Even though the flood extent uncertainty was not the main focus of the study, considering its relevance to the whole process of evaluation, this uncertainty was partially incorporated into the evaluation by contemplating different scenarios. We evaluated the impacts of the flood model uncertainties on the impacted population estimates using two different vulnerability scenarios designed according to the observed and simulated extent of the flood. It consisted in compensating the differences between simulated and real event flood extent in terms of the number of people exposed. We spatially increased and reduced the amount of population exposed in the buildings nearby areas where differences were observed between simulations and the real event. Taking these two scenarios into account, we noticed that the life-loss estimates were not significantly impacted by these uncertainties.

The comparison between the real accident records and the simulation results showed that, fortunately, the analysed case study demonstrated successful outcomes in terms of the alert and evacuation measures implemented. Despite the uncertainties identified in the models tested, the calibrated models were able to precisely evaluate economic damage and loss of life. It highlighted the great potential of these tools for preventive and planning development. Furthermore, the hypothetical scenarios of alert and evacuation allowed us to demonstrate that, as performed by Lumbroso et al. (2021), depending on the system's efficiency, flood consequences may have a significant increase or decrease. For the specific case study, loss of life could have been much more catastrophic. The simulated scenarios, exploring the inefficiency of flood alert and evacuation under poor conditions, revealed that life-loss could have reached the maximum rate of 3.5 % of the exposed population (pessimistic scenario) instead of the null actual life-loss recorded. Taking into account other uncertainty, we identified that life-loss could have reached the maximum rate of 8.7 %, considering the unknown scenario. The fragile circumstances that led to the successful evacuation in this case study, which relied on the actions of just one professional (the watchman), could have been turned into a much more catastrophic accident, highlighting the great importance of developing and implementing robust and secure alert systems for this kind of structure.

The estimates acquired throughout the development of this case study were adherent to observed data, which sustained the great potential of the use of these modelling technics for planning purposes. Besides, one of the great advantages of HEC-LifeSim is the possibility of dynamically simulating the evacuation of the population. The best suitability of this model in tailings dam failure events can be achieved by changing the model standards. Several criteria are editable, and changes in these criteria could assist in representing the physicochemical characteristics of the tailings. It is possible to adapt the representation of alert and evacuation to incorporate specific characteristics for a specific case (as we did in this work), and it is possible to change the life-loss rates to incorporate the impact of the debris and other characteristics of tailings in the contact human-fluid. In addition to HEC-LifeSim showing the ability to simulate the non-occurrence of fatalities like the one that occurred in the event, the model also made it possible to speculate on scenarios that take into account lower alert and evacuation efficiencies, which resulted in much more catastrophic scenarios in terms of loss of life.

450 Finally, this study explored models to estimate economic damage and loss of life in floods at the same event of tailings dam failure. In this sense, it shows the potential efficiency of the models currently widely used for flood simulation. A greater understanding of the application of these models in tailings flow can subsidize Brazilian and international legislation on dam safety by considering these consequences in risk assessments.

## Code and data availability

455 Code and data will be made available on request.

## Competing interests

The authors declare that they have no conflict of interest.

## Acknowledgments

The authors acknowledge the kind support provided by the Coordination of Superior Level Staff Improvement (CAPES), the
460 National Council for Scientific and Technological Development (CNPq), and the Foundation for Research Support of the State of Minas Gerais (FAPEMIG) for financial resources.

## References

ABEP: Critério de Classificação Econômica do Brasil. Dados com base no Levantamento Sócio Econômico 2010., São Paulo, Brazil, 2012.

465 Aboelata, M. and Bowles, D. S.: LIFESim: A Model for Estimating Dam Failure Life Loss, 274 pp., 2005.

Alabbad, Y., Yildirim, E., and Demir, I.: A web-based analytical urban flood damage and loss estimation framework, Environmental Modelling & Software, 163, 105670, https://doi.org/10.1016/j.envsoft.2023.105670, 2023.

Apel, H., Thieken, A. H., Merz, B., and Blochl, G.: Flood risk assessment and associated uncertainty, Natural Hazards and Earth System Science, 81, 343–347, https://doi.org/10.5194/nhess-9-289-2009, 2004.

470 Azam, S. and Li, Q.: Tailings dam failures: A review of the last one hundred years, Geotechnical News, 28, 50–53, https://doi.org/10.1373/clinchem.2008.105395, 2010.

Bernedo, C. E., Julien, P., and Leon, A.: Dam Breach Analysis in Tailings Storage Facilities (TSF), in: World Environmental and Water Resources Congress, 2216–2224, https://doi.org/10.1061/41173(414)231, 2011.

Bilali, A. El, Taleb, A., and Boutahri, I.: Application of HEC-RAS and HEC-LifeSim models for flood risk assessment, Journal
475 of Applied Water Engineering and Research, 0, 1–16, https://doi.org/10.1080/23249676.2021.1908183, 2021.

Bilali, A. El, Taleb, I., Nafii, A., and Taleb, A.: A practical probabilistic approach for simulating life loss in an urban area associated with a dam-break flood, International Journal of Disaster Risk Reduction, https://doi.org/10.1016/j.ijdrr.2022.103011, 2022.

Bombelli, I., Molinari, D., Asaridis, P., and Ballio, F.: The "Flood Damage Models" repository, in: IV European Conference on Flood Risk Management model, 6, https://doi.org/10.3311/floodrisk2020.11.3, 2021.

Brunner, G. W.: HEC-RAS. River Analysis System. Hydraulic Reference Manual - Version 6.0, U.S. Army Corps of Engineers, Davis, California, United States, 546 pp., 2021.

Dijkstra, E. W.: A Note on Two Problems in Connexion with Graphs, Numer. Math., 1, 269–271, 1959.

Fernandes, G. W., Goulart, F. F., Ranieri, B. D., Coelho, M. S., Dales, K., Boesche, N., Bustamante, M., Carvalho, F. A., Carvalho, D. C., Dirzo, R., Fernandes, S., Galetti, P. M., Millan, V. E. G., Mielke, C., Ramirez, J. L., Neves, A., Rogass, C., Ribeiro, S. P., Scariot, A., and Soares-Filho, B.: Deep into the mud: ecological and socio-economic impacts of the dam breach in Mariana, Brazil, Natureza e Conservação, 14, 35–45, https://doi.org/10.1016/j.ncon.2016.10.003, 2016.

Ge, W., Wang, X., Li, Z., Zhang, H., Guo, X., Wang, T., Gao, W., Lin, C., and van Gelder, P.: Interval Analysis of the Loss of Life Caused by Dam Failure, J Water Resour Plan Manag, 147, 04020098, https://doi.org/10.1061/(asce)wr.1943-5452.0001311, 2021.

Ge, W., Jiao, Y., Wu, M., Li, Z., Wang, T., Li, W., Zhang, Y., Gao, W., and van Gelder, P.: Estimating loss of life caused by dam breaches based on the simulation of floods routing and evacuation potential of population at risk, J Hydrol (Amst), 612, 128059, https://doi.org/10.1016/j.jhydrol.2022.128059, 2022.

Gerl, T., Kreibich, H., Franco, G., Marechal, D., and Schröter, K.: A review of flood loss models as basis for harmonization and benchmarking, PLoS One, 11, 1–22, https://doi.org/10.1371/journal.pone.0159791, 2016.

Gildeh, H. K., Halliday, A., Arenas, A., and Zhang, H.: Tailings Dam Breach Analysis: A Review of Methods, Practices, and Uncertainties, Mine Water Environ, 40, 128–150, https://doi.org/10.1007/s10230-020-00718-2, 2021.

Greenshields, B. D., Channing, W., and Miller, H.: A study of traffic capacity, in: XIV Annual Meeting of the Highway Research Board Held at Washington, 1935.

Guimarães, R. N., Moreira, V. R., Cruz, J. R. A., Saliba, A. P. M., and Amaral, M. C. S.: History of tailings dam failure: Impacts on access to safe water and influence on the legislative framework, Science of the Total Environment, 852, 158536, https://doi.org/10.1016/j.scitotenv.2022.158536, 2022.

Gutenson, J. L., Ernest, A. N. S., Oubeidillah, A. A., Zhu, L., Zhang, X., and Sadeghi, S. T.: Rapid flood damage prediction and forecasting using public domain cadastral and address point data with fuzzy logic algorithms, J Am Water Resour Assoc, 54, 104–123, https://doi.org/10.1111/1752-1688.12556, 2018.

Hellweger, F. and Maidment, D. R.: AGREE-DEM surface reconditioning system, Texas A&M University, Austin, Texas, United States, 1997.

Hill, P., Kavanagh, C., and Lang, S.: Applications of Simulation Model to Estimate Potential Loss of Life, in: XXVI International Congress on Large Dams, 2018.

510 Huang, D., Yu, Z., and Li, Y.: Calculation method and application of loss of life caused by dam break in China, Natural Hazards, 85, 39–57, https://doi.org/10.1007/s11069-016-2557-9, 2017.

IBGE: Descrição das variáveis da amostra do Censo Demográfico 2010, Rio de Janeiro, Brazil, 1–62 pp., 2011.

IBGE: Grade Estatística, Rio de Janeiro, Brazil, 31 pp., 2016.

ICOLD: Risk of Dangerous Occurrences, Lessons Learnt from Practical Experiences, Bulletin 121, Paris, France, 146 pp., 515 2001.

Jarihani, A. A., Callow, J. N., McVicar, T. R., Van Niel, T. G., and Larsen, J. R.: Satellite-derived Digital Elevation Model (DEM) selection, preparation and correction for hydrodynamic modelling in large, low-gradient and data-sparse catchments, J Hydrol (Amst), 524, 489–506, https://doi.org/10.1016/j.jhydrol.2015.02.049, 2015.

Jeyapalan, B. J. K., Duncan, M., and Seed, B.: Investigation of flow failures of tailings dams, Journal of Geotechnical and 520 Geoenvironmental Engineering, 109, 172–189, https://doi.org/10.1061/(ASCE)0733-9410(1983)109:2(172), 1983.

Jiao, H., Li, W., and Ma, D.: Assessment of life loss due to dam breach using improved variable fuzzy method, Sci Rep, 12, 1–7, https://doi.org/10.1038/s41598-022-07136-0, 2022.

Jin, M. and Fread, D. L.: 1D Modeling of Mud/Debris Unsteady Flows, Journal of Hydraulic Engineering, 125, 827–834, https://doi.org/10.1061/(ASCE)0733-9429(1999)125:8(827), 1999.

525 Jongejan, R. B., Jonkman, S. N., and Vrijling, J. K.: Methods for the economic valuation of loss of life, in: Conference on International Law and Management of Large-Scale Risks, 8, 2005.

Jonkman, S. N., Van Gelder, P. H. A. J. M., and Vrijling, J. K.: An overview of quantitative risk measures for loss of life and economic damage, J Hazard Mater, 99, 1–30, https://doi.org/10.1016/S0304-3894(02)00283-2, 2003.

Jonkman, S. N., Vrijling, J. K., and Vrouwender, A. C. W. M.: Methods for the estimation of loss of life due to floods: a 530 literature review and a proposal for a new method, Natural Hazards, 46, 353–389, https://doi.org/10.1007/s11069-008-9227-5, 2008.

Jonkman, S. N., Maaskant, B. B., Kolen, B. B., and Needham, J. T. J.: Loss of life estimation - Review, developments and challenges, in: III European Conference on Flood Risk Management, https://doi.org/10.1051/e3sconf/20160706004, 2016.

Kalinina, A., Spada, M., and Burgherr, P.: Alternative life-loss rates for failures of large concrete and masonry dams in 535 mountain regions of OECD countries, in: XXVIII International European Safety and Reliability Conference, ESREL 2018, 9, https://doi.org/10.1201/9781351174664-213, 2018.

Kalinina, A., Spada, M., and Burgherr, P.: Quantitative Assessment of Uncertainties and Sensitivities in the Estimation of Life Loss Due to the Instantaneous Break of a Hypothetical Dam in Switzerland, Water (Basel), 13, 22, https://doi.org/10.3390/w13233414, 2021.

540 Kolen, B., Dannenberg, P., and Gelder, P. van: Quantitative assessment of evacuation measures in flood-prone areas, in: IV European Conference on Flood Risk Management, 5, https://doi.org/10.3311/floodrisk2020.19.6, 2020.

Kossoff, D., Dubbin, W. E., Alfredsson, M., Edwards, S. J., Macklin, M. G., and Hudson-edwards, K. A.: Mine tailings dams: Characteristics, failure, environmental impacts, and remediation, Applied Geochemistry, 51, 229–245, https://doi.org/10.1016/j.apgeochem.2014.09.010, 2014.

545 Larrauri Concha, P. and Lall, U.: Tailings Dams Failures: Updated Statistical Model for Discharge Volume and Runout, Environments, 5, 10, https://doi.org/10.3390/environments5020028, 2018.

Leong-Cuzack, T., Nielsen, C., Kavanagh, C., and Watt, S.: Quantitative Assessment of Dam Safety Emergency Management Using HEC-LifeSim: Is it feasible?, in: ANCOLD Conference, 11, 2019.

Li, W., Li, Z., Ge, W., and Wu, S.: Risk Evaluation Model of Life Loss Caused by Dam-Break Flood and Its Application, 550 Water (Basel), 11, 1–12, https://doi.org/10.3390/w11071359, 2019.

Lumbroso, D. and Davison, M.: Use of an agent-based model and Monte Carlo analysis to estimate the effectiveness of emergency management interventions to reduce loss of life during extreme floods, J Flood Risk Manag, 11, S419–S433, https://doi.org/10.1111/jfr3.12230, 2018.

Lumbroso, D., Davison, M., Body, R., and Petkovšek, G.: Modelling the Brumadinho tailings dam failure, the subsequent loss 555 of life and how it could have been reduced, Natural Hazards and Earth System Sciences, 21, 21–37, https://doi.org/10.5194/nhess-21-21-2021, 2021.

Machado, N. C.: Retroanálise da propagação decorrente da ruptura da barragem do fundão com diferentes modelos numéricos e hipóteses de simulação, Dissertation, Federal University of Minas Gerais, Belo Horizonte, Minas Gerais, Brazil, 159 pp., 2017.

560 Mahmoud, A. A., Wang, J. T., and Jin, F.: An improved method for estimating life losses from dam failure in China, Stochastic Environmental Research and Risk Assessment, 34, 1263–1279, https://doi.org/10.1007/s00477-020-01820-1, 2020.

Martin, V., Ph, D., Eng, P., Fontaine, D., Eng, P., Cathcart, J., Ph, D., and Eng, P.: Challenges with conducting tailings dam breach studies, in: Tailings and Mine Waste 2015, 15, https://doi.org/10.14288/1.0320883, 2015.

McClelland, D. M. and Bowles, D. S.: Estimating life loss for dam safety risk assessment - A review and new approach, 565 Institute for Water Resources U.S. Army Corps of Engineers, 420 pp., 2002.

Melo, L. P. R. de: Análise comparativa de metodologias de previsão de inundação decorrente da ruptura de barragens de rejeitos: caso hipotético da barragem Tico-Tico, Dissertation, Federal University of Minas Gerais, Belo Horizonte, Minas Gerais, Brazil, 183 pp., 2013.

Merz, B., Kreibich, H., Schwarze, R., and Thieken, A.: Review article "assessment of economic flood damage," Natural 570 Hazards and Earth System Science, 10, 1697–1724, https://doi.org/10.5194/nhess-10-1697-2010, 2010.

Molinari, D., De Bruijn, K. M., Castillo-Rodríguez, J. T., Aronica, G. T., and Bouwer, L. M.: Validation of flood risk models: Current practice and possible improvements, International Journal of Disaster Risk Reduction, 33, 441–448, https://doi.org/10.1016/j.ijdrr.2018.10.022, 2019.

Nascimento, N., Machado, L. M., Silva, A., Baptista, M., Lima, J. L., Gonçalves, M., Silva, A., Dias, R., and Machado, É.: Flood-damage curves: Methodological development for the Brazilian context, Water Pract Technol, 1, https://doi.org/10.2166/wpt.2006022, 2006.

Nascimento, N., Machado, L. M., Baptista, M., and De Paula, A.: The assessment of damage caused by floods in the Brazilian context, Urban Water J, 4, 195–210, https://doi.org/10.1080/15730620701466591, 2007.

Needham, J., Fields, W., and Lehman, W.: The US Army Corps of Engineers Scalable Approach to Estimating Loss of Life from Flooding, in: III European Conference on Flood Risk Management, 6, https://doi.org/10.1051/e3sconf/20160706003, 2016.

NRCS: National Engineering Handbook: Part 360, Hydrology, Washington DC, United States, 1997.

NRCS: Manning's n Values for Various Land Covers to Use for Dam Breach Analyses by NRCS in Kansas, 2016.

O'Brien, J. S. and Julien, P. Y.: Physical properties and mechanics hyperconcentrated sediment flows, in: Specialty Conference - Delineation of Landslide, Flash Flood and Debris Flow Hazards in Utah, 1985.

Paiva, R. C. D., Collischonn, W., and Tucci, C. E. M.: Large scale hydrologic and hydrodynamic modeling using limited data and a GIS based approach, J Hydrol (Amst), 406, 170–181, https://doi.org/10.1016/j.jhydrol.2011.06.007, 2011.

Piciullo, L., Storrøsten, E. B., Zhongqiang, L., Farrokh, N., and Lacasse, S.: A new look at the statistics of tailings dam failures, Eng Geol, 303, 106657, https://doi.org/10.1016/j.enggeo.2022.106657, 2022.

Pimenta de Ávila: Relatório sobre a ruptura da barragem de São Francisco, da mineração Rio Pomba Cataguases, situada em Miraí, MG. FE-100-RL-111318-00, 2007.

Proske, D.: Comparison of dam failure frequencies and failure probabilities, Beton- und Stahlbetonbau, 113, 2–6, https://doi.org/10.1002/best.201800047, 2018.

RESCDAM: Rescue Actions Based on Dam-Break Flood Analysis. The Use of Physical Models in Dam-Break Flood Analysis, Helsinki, Finland, 2000.

Rico, M., Benito, G., and Díez-Herrero, A.: Floods from tailings dam failures, J Hazard Mater, 154, 79–87, https://doi.org/10.1016/j.jhazmat.2007.09.110, 2008a.

Rico, M., Benito, G., Salgueiro, A. R., Díez-Herrero, A., and Pereira, H. G.: Reported tailings dam failures. A review of the European incidents in the worldwide context, J Hazard Mater, 152, 846–852, https://doi.org/10.1016/j.jhazmat.2007.07.050, 2008b.

Risher, P., Ackerman, C., Morrill-Winter, J., Fields, W., and Needham, J.: Levee Breach Consequence Model Validated by Case Study in Joso, Japan, in: X Association of State Dam Safety Conference, 13, 2017.

Rocha, F. F.: Retroanálise da ruptura da barragem São Francisco – Miraí, Minas Gerais, Brasil, Dissertation, Federal University of Minas Gerais, Dissertation. Engineering School, Federal University of Minas Gerais, Belo Horizonte, Minas Gerais, Brazil, 184 pp., 2015.

Rogers, G. O. and Sorensen, J.: Warning and response in two hazardous materials transportation accidents in the U.S., J Hazard Mater, 22, 57–74, https://doi.org/https://doi.org/10.1016/0304-3894(89)85028-9, 1989.

Rotta, L. H. S., Alcântara, E., Park, E., Negri, R. G., Lin, Y. N., Bernardo, N., Mendes, T. S. G., and Souza Filho, C. R.: The 2019 Brumadinho tailings dam collapse: Possible cause and impacts of the worst human and environmental disaster in Brazil, International Journal of Applied Earth Observation and Geoinformation, 90, 102–119, https://doi.org/10.1016/j.jag.2020.102119, 2020.

Saksena, S. and Merwade, V.: Incorporating the effect of DEM resolution and accuracy for improved flood inundation mapping, J Hydrol (Amst), 530, 180–194, https://doi.org/10.1016/j.jhydrol.2015.09.069, 2015.

Silva, A. F. R. da, Eleutério, J. C., and Nascimento, N. D. O.: Alerta e Redução de Perdas de Vidas Associadas à Ruptura Hipotética da Barragem da Pampulha - MG, in: XXIV Brazilian Water Resources Symposium, 10, 2021.

Sorensen, J. and Mileti, D.: First Alert and/or Warning Issuance Time Estimation for Dam Breaches, Controlled Dam Releases, and Levee Breaches or Overtopping, 48 pp., 2015a.

Sorensen, J. and Mileti, D.: First Alert or Warning Diffusion Time Estimation for Dam Breaches, Controlled Dam Releases and Levee Breaches or Overtopping, 56 pp., 2015b.

Sorensen, J. and Mileti, D.: Influence Weights and Measures for the Factors Shaping First Alert/Warning Delay, Diffusion and Protective Action Initiation Curves for Dam Breaches , Controlled Dam Releases , and Levee Breaches or Overtopping, 9 pp., 2015c.

Sorensen, J. and Mileti, D.: INTERVIEW SCHEDULE. Community Warning Issuance, Diffusion, and Protective Action Initiation Estimation, 12 pp., 2015d.

Sorensen, J. and Mileti, D.: Protective Action Initiation Time Estimation for Dam Breaches, Controlled Dam Releases, and Levee Breaches or Overtopping, 51 pp., 2015e.

STJ: Recurso Especial nº 1.374.284 – MG (2012/0108265-7). Relator Ministro Luis Felipe Salomão, Brasilia, Brazil, 2014.

Tomura, S., Chiba, M., Yamamoto, T., Uemura, F., Masuya, S., Omura, N., Yoshida, T., Takeda, A., Hoshino, T., Yamada, T., and Nakatsugawa, M.: Fatality estimation by life loss evaluation model for the large-scale floods under future climate, 22nd Congress of the International Association for Hydro-Environment Engineering and Research-Asia Pacific Division, IAHR-APD 2020: "Creating Resilience to Water-Related Challenges," 1–8, 2020.

Tonn, G. L. and Guikema, S. D.: An Agent-Based Model of Evolving Community Flood Risk, Risk Analysis, 38, 1258–1278, https://doi.org/10.1111/risa.12939, 2018.

Travis, B., Teal, M., and Gusman, J.: Best methods and inherent limitations of bulked flow modeling with HEC-RAS, in: World Environmental and Water Resources Congress, 1995–1202, https://doi.org/10.1061/9780784412312.121, 2012.

USACE: United States Army Corps of Engineers. Business Depth Damage Analysis Procedure, Research Report 85-R-5, Alexandria, Virginia, United States, 1985.

USACE: HEC-LifeSim. Life Loss Estimation. User's Manual - Version 1.0.1, 216 pp., 2018a.

USACE: United States Army Corps of Engineers. HEC-LifeSim. Version 1.01. Hydrologic Engineering Center. Davis, California, United States, 2018b.

USACE: LifeSim. Version 2.0. Hydrologic Engineering Center. Davis, California, United States, 2021.

USGS: Landsat 5 TM 2005-15-10, https://earthexplorer.usgs.gov, 2005.

Veizaga, F. M., De Paes, R. P., Eleutério, J., Rocha, F. F., and Palmier, L. R.: Modelagem hidráulica de inundação e estimativa de danos diretos causados por rompimento real da barragem São Francisco, Miraí, Minas Gerais, in: XXII Brazilian Water

645    Resources Symposium, 8, 2017.

Wang, H.: Lessons Learnt From Evacuation Modelling for Dam Failure Consequence Assessments, in: ANCOLD Conference, 9, 2019.

Project Chronology of Major Tailings Dam Failures: http://www.wise-uranium.org/mdaf.html, last access: 25 March 2023.

Yamazaki, D., Baugh, C. A., Bates, P. D., Kanae, S., Alsdorf, D. E., and Oki, T.: Adjustment of a spaceborne DEM for use in

650    floodplain hydrodynamic modeling, J Hydrol (Amst), 436–437, 81–91, https://doi.org/10.1016/j.jhydrol.2012.02.045, 2012.

Zhuo, L. and Han, D.: Agent-based modelling and flood risk management: A compendious literature review, J Hydrol (Amst), 591, https://doi.org/10.1016/j.jhydrol.2020.125600, 2020.